Journal of Thermal Analysis and Calorimetry, Vol. 82 (2005) 659–664

KINETIC ANALYSES USING SIMULTANEOUS TG/DSC MEASUREMENTS
Part II: Decomposition of calcium carbonate having different particle sizes

J. P. Sanders[1*] *and P. K. Gallagher*[2]

[1]The National Brick Research Center, Clemson University,100 Clemson Research Blvd., Anderson, SC 20625
[2]Adjunct Prof., Clemson Univ. - Emeritus Prof., The Ohio State Univ. USA

The thermal decomposition of $CaCO_3$ was studied using simultaneous TG/DSC for two different ranges of particle size from the same source and a physical mixture of each. The difference in kinetic behavior was as expected qualitatively, but significantly different quantitatively. In addition, the mixture did not behave as a simple combination of its end members. These discrepancies are attributed to the problems associated with mass and thermal transport. The TG data again proved easier to fit than the DSC data.

Keywords: *activation energy, Arrhenius kinetic parameters, calcium carbonate, DSC, particle size, TG, thermal decomposition*

Introduction

This work was undertaken in order to compare, under identical conditions, Arrhenius kinetic parameters for the decomposition of calcium carbonate from the same source, but having distinctly different particle sizes. The initial, perhaps naïve, assumption is that the mechanism and activation energy would be the same and that the difference in rate would be indicated by a larger pre-exponential or log A term for the material having the smaller particle size. Consider the contracting geometry mechanisms, which have occasionally been applied to this decomposition [1]. In the derivation of the rate equation, for the contracting geometry mechanism, the rate constant, k, is the presumed constant rate of interface motion divided by the particle radius, r. Consequently, the Arrhenius plots for different particle sizes should be parallel, but displaced from each other by ($\log r_1 - \log r_2$). Similarly, if the reaction proceeds in an uncomplicated manner, the kinetics observed for a mixture of two particle sizes should be a simple composite, in the proper proportions, of the kinetics observed for the separate particle sizes.

These presumptions are predicated on a traditional interpretation of Arrhenius parameters based on homogeneous kinetics, i.e., the activation energy, E, resulting from that needed for the chemical bond rearrangement process and the pre-exponential term, A, arising from the probability of the reactive configuration or site. Much controversy arises when these interpretations are extrapolated from homogeneous to heterogeneous conditions, as in the preceding paragraph. Such justified criticisms have been well summarized in the recent critical tutorial review by Galwey [2]. The ready reversibility of the calcium carbonate decomposition and its strongly endothermic nature have added further complexities associated with mass and thermal transport conditions (see for example [1, 3]). The rate of the decomposition can become controlled by the supply of heat to the reaction zone and/or the effectiveness of the sweep gas in removing the reversible product(s) from the immediate reaction environment.

Because of the immense technological importance of this reaction and because of its simplistic stoichiometry, (Eq. (1)) $CaCO_3$ has been extensively studied and thus serves as a well documented test case. Indeed, it was recently selected by the Kinetics Committee of the International Confederation of Thermal Analysis and Calorimetry (ICTAC) as a model system to compare methods of numerical analysis for kinetic data [4]. However, if complications arise from the mass and thermal transport conditions, these straightforward initial predictions will not be the result. In addition to testing those aspects, the method used for numerical analysis of the data will be evaluated to see how the results for the mixture are best fitted, i.e., as simultaneous, sequential or a single reaction(s).

$$CaCO_{3(s)} \leftrightarrow CaO_{(s)} + CO_{2(g)} \quad (1)$$

Experimental procedures

The source of $CaCO_3$ was a single crystal of calcite obtained from the Sargent-Welch Scientific Com-

* Author for correspondence: jpsand@clemson.edu

1388–6150/$20.00
© 2005 Akadémiai Kiadó, Budapest
Akadémiai Kiadó, Budapest, Hungary
Springer, Dordrecht, The Netherlands

pany. A large piece was crushed and ground in an alumina mortar and pestle. Two size-fractions were isolated by sieving. The coarser fraction was 149 to 74 μm and the finer fraction was <44 μm. A third sample was prepared by thoroughly mixing equal amounts of both particle sizes. After the size fractions were separated by sieving, the samples were dried at 110°C for 24 h and then stored in a desiccator prior to use.

Simultaneous thermogravimetric/differential scanning calorimetery (TG/DSC) measurements were performed on a Netzsch 449C simultaneous thermal analyzer using open alumina crucibles. The nominal sample size used in this work was 10 mg (±0.5 mg). An argon atmosphere flowing at 100 mL min^{-1} was used for all measurements. Heating rates of 2, 4, 8, 16, and 32°C min^{-1} were used in this study. Baselines and sensitivity calibrations were obtained for each heating rate. An empty alumina crucible was used as the reference for the DSC measurements. The sensitivity calibration calculations for the DSC measurements were made using measurements on sapphire disks.

Data analysis was performed using Netzsch's Proteus and Thermokinetic 2 software packages [5]. In the least-squares fitting of the TG data no weighting factors were applied. For the DSC data, tangential baselines were fitted to the endothermic decomposition and a weighting factor of w=1/(abs(Y_{max})+abs(Y_{min})) was applied. For each data set, single-step linear regression was performed as well as multi-step non-linear regression analysis using simultaneous reactions.

Further, a 5 mg sample of high purity (99.997%) Al foil from Alfa AESAR was heated at 8°C min^{-1} in argon to determine the temperature dependence and thermal resistance associated with the measurement configuration. These correction parameters are used to account for distortion of the DSC signal associated with the thermal transport properties of the crucible and measuring-head materials as well as the interfacial transport between the sample and the crucible and the crucible and the measuring-head.

Results and discussion

Comparisons of the TG and DSC measurements for the samples heated at the intermediate rate of 8ºC min^{-1} in argon for each of the size fractions are provided in Figs 1 and 2 respectively. Similarly a comparison of the DTG data at 8ºC min^{-1} is given in Fig. 3. A summary of onset, endset and peak data for the TG, DTG and DSC data reported in Figs 1–3 is given in Table 1.

As would be expected, the finest size-fraction, <44 μm, displayed the lowest onset and endset temperatures for the TG data while the coarser fraction displayed the highest onset and endset temperatures. In short, the curves for the two size-fractions appear to have the same shape with different onset temperatures. The TG curve for the blended sample,

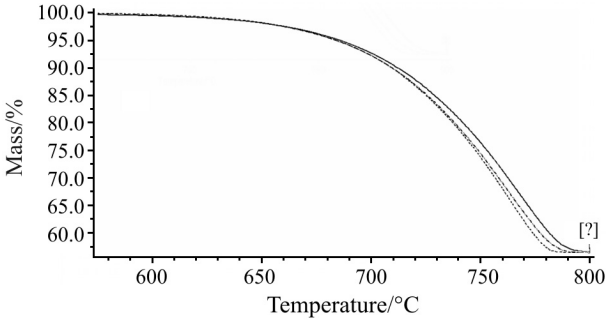

Fig. 1 TG measurements at 8ºC min^{-1} in argon for the three size-fractions of $CaCO_3$; —— – 149–74 μm fraction, - - - – <44 μm fraction, -···-·- – Blend

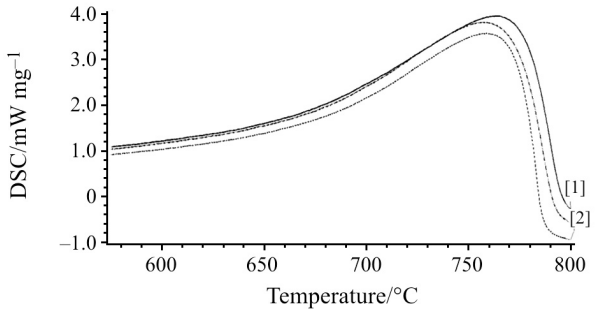

Fig. 2 DSC measurements at 8ºC min^{-1} in argon for the three size-fractions of $CaCO_3$; —— – 149–74 μm fraction, - - - – <44 μm fraction, -···-·- – blend

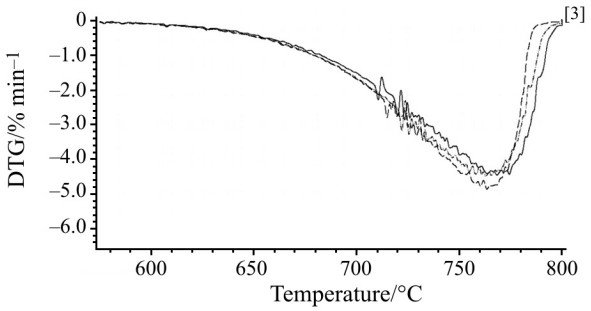

Fig. 3 DTG measurements at 8°C min^{-1} in argon for the three size-fractions of $CaCO_3$; —— – 149–74 μm fraction, - - - – <44 μm fraction, -···-·- – blend

Table 1 Onset and peak data for TG, DSC and DTG measurements at 8°C min^{-1} in argon

Size fraction	TG onset/°C	TG endset/°C	DSC peak/°C	DTG peak/°C
149–74 μm	715	786	764	768
blend	713	782	757	763
<44 μm	712	779	759	764

however, took on a somewhat unexpected shape. The onset of carbonate decomposition for the blended sample is very similar to the finer fraction and the endset for the blended sample is more similar to the coarser size-fraction. The end result is a curve with a stretched appearance with an onset similar to the finer size-fraction and an endset similar to the coarser size-fraction. It does not appear, however, that the curves for the mixed sample can be recreated by the simple addition of equal proportions of the curves for the end members. Neither the DSC curves in Fig. 2 nor the DTG curves in Fig. 3 for the mixture appear to exhibit the proper structure for combining the end members. Similarly, the TG curve for the blended sample exhibits a different rate of decomposition (slope) than either of the finer or the coarser size fractions. Clearly the transport properties and potential re-crystallization have become factors.

Neither the DSC curves in Fig. 2, nor the DTG curves in Fig. 3, for the mixture appear to exhibit the proper structure for combining the end members. Because of the slightly different decomposition rate for the blended sample, both the DTG and DSC peaks have a slightly different appearance from the coarse and fine size fractions. This difference in peak shape is likely the source of the apparent inconsistency in the relationship of the peak temperatures seen in Table 1 for the DSC and DTG peaks.

A sample data set for the finer size-fraction is given in Figs 4 and 5 for TG and DSC respectively. The heating rates used in this investigation are indicated in each figure. A variety of kinetic analyses were performed on these data.

As a first step in the kinetic modeling of the data, a simple linear regression was performed on the TG and DSC data from each size fraction. In this analysis, the Thermokinetics software was allowed to pick the model and determine the kinetic parameters that best fitted the selected model. With this type of analysis, the software tends to pick the model with the most parameters in order to provide the best fit. A summary of the results of this analysis is provided in Table 2. For all three size fractions an n^{th} order Prout Tompkins model with autocatalysis was selected by

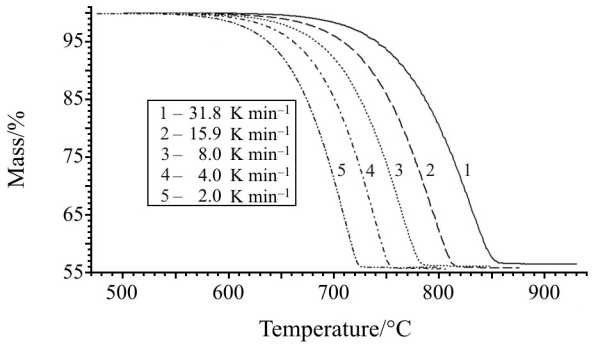

Fig. 4 TG curves at different heating rates the finer (<44 μm) size-fraction

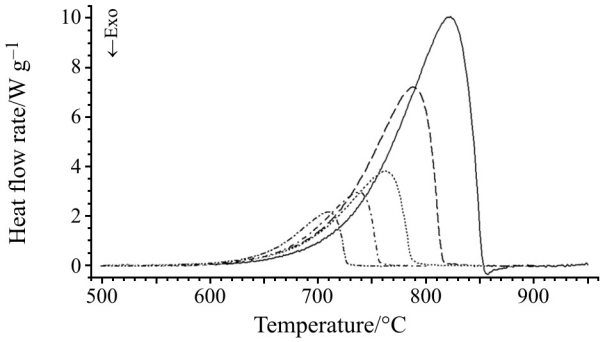

Fig. 5 DSC curves at different heating rates the finer (<44 μm) size-fraction

the software to fit the TG data. This model has four fitting parameters which include the pre-exponential factor, the activation energy, the reaction order, and the autocatalysis factor. For each size fraction the fit, R^2, was greater than 0.999, but the contribution from catalysis is extremely small, less than 0.07.

For the DSC data, an n^{th} order model with autocatalysis was selected by the linear-regression fitting of the software. This model also has four parameters for fitting and, for each size fraction, the fit, R^2, was greater than 0.995. As described in the earlier work, the TG data gave superior results for the reasons described in Part I [6]. The autocatalysis factor used to model the DSC data for each of the size frac-

Table 2 Arrhenius kinetic parameters from linear-regression fitting of the thermal decomposition of $CaCO_3$ in argon

Size fraction	Data type	Model	E/kJ mol^{-1}	log$A$/s^{-1}	Order/autocatalysis factor	R^2
149–74 μm	TG	Prout-Tompkins n^{th} order with autocatalysis	194	7.23	$0.44/4.03\cdot10^{-2}$	0.9998
blend	TG		194	7.30	$0.47/6.24\cdot10^{-2}$	0.9998
<44 μm	TG		191	7.13	$0.39/7.08\cdot10^{-2}$	0.9993
149–74 μm	DSC	n^{th} order with autocatalysis	199	7.44	0.50/–0.30	0.9962
blend	DSC		199	7.47	0.54/–0.19	0.9968
<44 μm	DSC		194	7.21	0.46/–0.17	0.9954

tions was negative (–0.17 to –0.30). The lack of significant contribution from the autocatalysis factors used to fit both the TG and DSC data seem to invalidate the use of these models. It appears that the high degree of fit provided by these models was due to the availability of extra fitting parameters in the model chosen by the software. The best fit model selection, based on the software used, was the same as what was that observed in Part I of this study [6].

There are, however, mechanisms with fewer adjustable parameters that fit almost as well and also allow more direct testing of the premise regarding the variation of E and A with particle size. A summary of these results is presented in Table 3. A simple n^{th} order model fits both the TG and the DSC data quite well. The average value of activation energy, E, was 194 kJ mol^{-1} for the TG data and 200 kJ mol^{-1} for the DSC data. A very small range of activation energy was observed. The optimum reaction order, n, varied from 0.27 to 0.38 for the TG data and 0.30 to 0.40 for the DSC data. The values of the pre-exponential factor, log$A$, are seen to peak for the mixture and the larger values of log$A$ are associated with the higher values of E for all results. Due to the range of reaction orders, it was not possible to clearly discern a trend in the pre-exponential term as a function of size fraction. To further simplify the kinetic analysis and comparison, the order of the reaction was fixed at 0.333 which approximates the contracting geometry mechanism. In this case the average activation energy was found to be 194 kJ mol^{-1} for the TG data and 198 kJ mol^{-1} for the DSC data.

To determine the variation of log$A$ with particle size exclusively, kinetic fitting to the n^{th} order equation was done using a fixed order of 0.333 and the average value of E appropriate for that data set. A summary of these results is given in Table 4. The quality of the data fit for the TG data is represented graphically in Figs 6 through 8 for the coarser size-fraction, blend, and finer-size fractions, respectively while the DSC data fit is displayed in Figs 9 through 11, respectively. The quality of fit indicated in Figs 6 through 11 for each of the size fractions and the results summarized in Table 4 support this simple evaluation. Only the very end of the reaction at the highest heating rate shows much departure for the DSC data in Figs 9 through 11. The correlation coefficients, R^2, for the TG data are all >0.999, while the DSC data are fitted to >0.99. A general trend of increasing pre-exponential term, log$A$, was found with decreasing particle size for both the TG and DSC data. This is in agreement with the expected trend described in the introduction.

Table 4 summarizes the results using the contracting-sphere model suggested in the introduction,

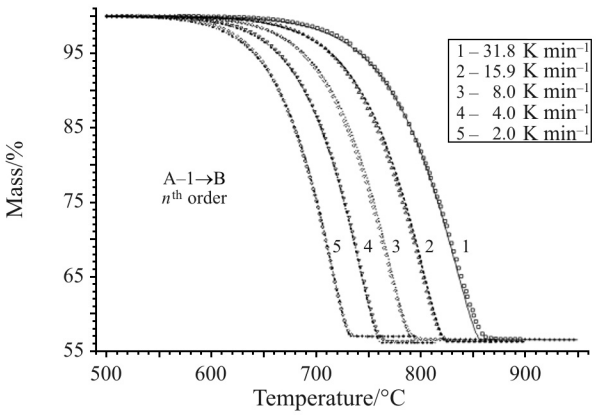

Fig. 6 Kinetic model fit for TG data for the thermal decomposition of the coarser (149–47 μm) size-fraction using an n^{th} order model with n=0.333 and E=194 kJ mol^{-1} (symbols represent the experimental data and lines are result of model calculations)

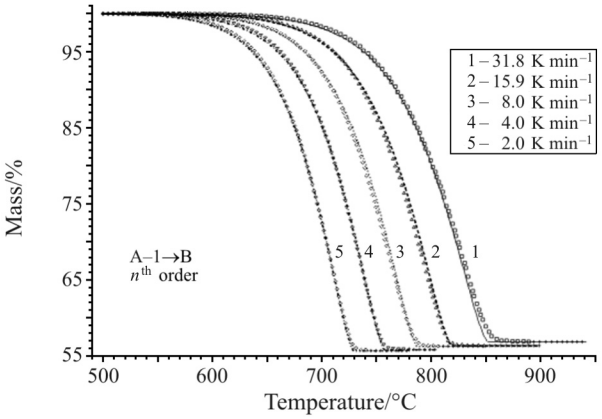

Fig. 7 Kinetic model fit for TG data for the thermal decomposition of the size-fraction blend using an n^{th} order model with n=0.333 and E=194 kJ mol^{-1} (symbols represent the experimental data and lines are result of model calculations)

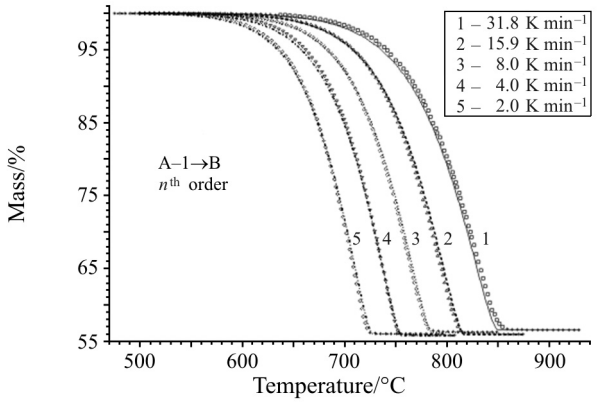

Fig. 8 Kinetic model fit for TG data for the thermal decomposition of the finer size-fraction using an n^{th} order model with n=0.333 and E=194 kJ mol^{-1} (symbols represent the experimental data and lines are result of model calculations)

Table 3 Arrhenius kinetic parameters for the thermal decomposition of $CaCO_3$ in Ar using the n^{th} order model

Size fraction	Data type	Model	E/kJ mol^{-1}	log$A$/s^{-1}	Order, n	R^2
149–74 μm	TG		195	7.23	0.38	0.9998
blend	TG	n^{th} order	195	7.29	0.37	0.9997
<44 μm	TG		192	7.11	0.27	0.9992
149–74 μm	DSC		201	7.57	0.38	0.9949
blend	DSC	n^{th} order	202	7.68	0.40	0.9944
<44 μm	DSC		196	7.38	0.31	0.9917

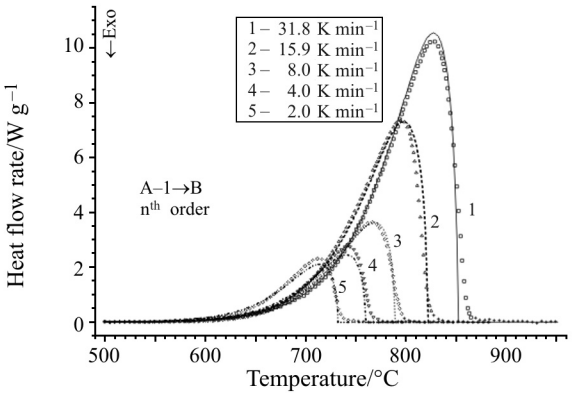

Fig. 9 Kinetic model fit for DSC data for the thermal decomposition of the coarser (149·47 μm) size-fraction using an n^{th} order model with n=0.333 and E=198 kJ mol^{-1} (symbols represent the experimental data and lines are result of model calculations)

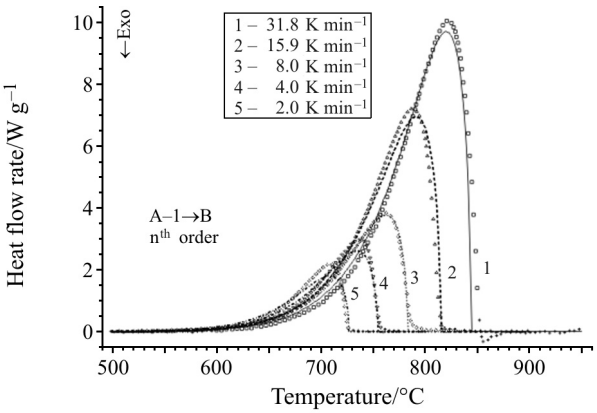

Fig. 11 Kinetic model fit for TG data for the thermal decomposition of the finer size-fraction using an n^{th} order model with n=0.333 and E=194 kJ mol^{-1} (symbols represent the experimental data and lines are result of model calculations)

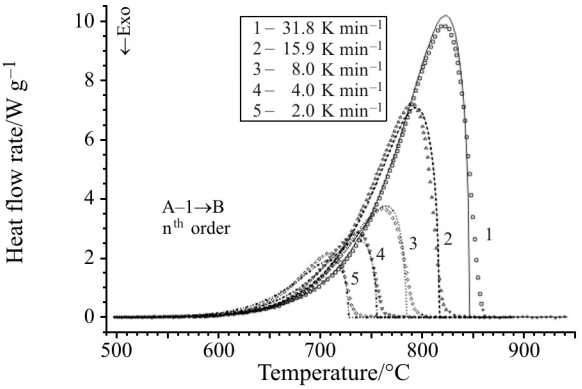

Fig. 10 Kinetic model fit for DSC data for the thermal decomposition of the size-fraction blend using an n^{th} order model with n=0.333 and E=198 kJ mol^{-1} (symbols represent the experimental data and lines are result of model calculations)

but which fits this data less well. If an average value of 112 μm is assumed for the larger particle size and a value of 30 μm is used for the smaller particle size, then the difference in log$A$ for the two particle sizes should be 0.6, an order of magnitude greater than that observed for the more reliable TG results. Again the mixture with its wide range of particle sizes exhibits the larger value of log A. This is further evidence that the simple view of the reaction mechanism requires severe modification.

After only a small amount of the sample has decomposed, sufficient CO_2 is formed to fill the crucible as well as the pores and interstices of the sample. Because the reaction is reversible, this raises the equilibrium decomposition temperature substantially, depending upon the effectiveness of the flowing atmosphere. As a consequence, the individual particle-size becomes much less of a factor. The sample pile effectively approaches a single particle as it reacts from the exterior inward towards the central core. This behavior has been noted in other reversible reactions, e.g., the dehydration of $Li_2SO_4{\cdot}0.5H_2O$ [7]. A possible confirmation of this effect would be to run the mixture under the two extremes of atmosphere, pure CO_2 or vacuum. In a CO_2 atmosphere, both decompositions would shift to a common higher temperature. Under vacuum, they would shift to a lower temperature and separate more distinctly.

Figure 12 shows the DTG curves for such experiments at 8ºC min^{-1}. The shift in temperature with P_{CO2} is obvious. The decreased resolution as a function of particle size is evident in CO_2, but the enhanced resolution in vacuum is very marginal, if at all. The effectiveness

Table 4 Arrhenius kinetic parameters for the thermal decomposition of $CaCO_3$ in argon using the contracting-sphere the rate law, $kt=1-(1-\alpha)^{0.333}$ with activation energy fixed

Size fraction	Data type	Model	E/kJ mol^{-1}	log$A$/s^{-1}	Order, n	R^2
149–74 μm	TG		194	7.17	0.333	0.9997
blend	TG	n^{th} order	194	7.21	0.333	0.9997
<44 μm	TG		194	7.23	0.333	0.9990
149–74 μm	DSC		198	7.41	0.333	0.9932
blend	DSC	n^{th} order	198	7.46	0.333	0.9910
<44 μm	DSC		198	7.48	0.333	0.9914

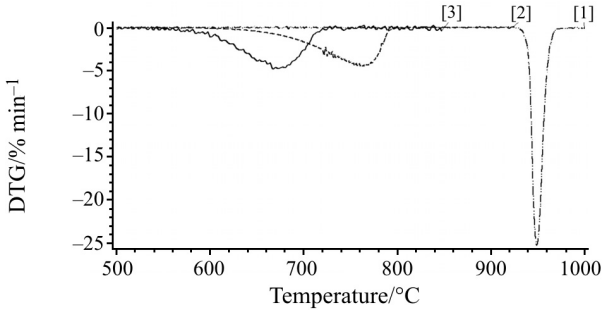

Fig. 12 DTG measurements for the blend at 8°C min^{-1} in various atmosphere; — – vacuum, ---- – argon, -···- CO_2

of the vacuum for completely removing the CO_2 from the reacting interface may be in question.

Another goal of this work was to see how the software would treat the decomposition of the mixed particle size sample, as sequential or consecutive reactions? The results in Tables 3 and 4, however, show that the mixed reaction is fitted with a single reaction scheme, as well as or better than the individual fractions. Attempts to fit it as a two-stage reaction confirmed this with the second stage representing only the last approximately ten percent of the reaction rather than equal divisions of the overall reaction.

Conclusions

- The intuitive effects of particle size on the Arrhenius parameters for the thermal decomposition of $CaCO_3$ are suppressed by the mass transport aspects of this readily reversible reaction.
- In a flowing neutral atmosphere the differences observed between the reaction kinetics are much less pronounced than would be expected for different particle size fractions.
- An equal mixture of two distinctly different particle size fractions does not decompose as would be predicted from a simple addition of the separate decompositions.
- This behavior is attributed to a saturation of the reaction zone with the gaseous decomposition product. The reversible nature of the reaction then causes the sample to decompose as though it was a single large particle at a rate dependent on the mass transport situation.

As was observed earlier, TG data are fitted with significantly greater precision than are DSC data and there is not a direct superposition of DTG and DSC curves [6, 8].

References

1 P. K. Gallagher and D. W. Johnson, Jr., Thermochim. Acta, 6 (1973) 67.
2 A. K. Galwey, Thermochim. Acta, 423 (2004) 139.
3 M. Maciejewski, J. Thermal Anal., 51 (1992) 33.
4 M. Brown *et al*., Thermochim. Acta, 355 (2000) 125.
5 J. Opffermann, J. Therm. Anal. Cal., 60 (2000) 641.
6 J. P. Sanders and P. K. Gallagher, Thermochim. Acta, 388 (2002) 115.
7 J. Huang and P. K. Gallagher, Thermochim. Acta, 192 (1991) 35.
8 J. P. Sanders and P. K. Gallagher, J. Therm. Anal. Cal., 72 (2003) 777.

DOI: 10.1007/s10973-005-6917-z